Identification of Acceptor Substrate Binding Subsites +2 and +3 in the Amylomaltase from *Thermus thermophilus* HB8†

Thijs Kaper,[‡,§,||] Hans Leemhuis,[§] Joost C. M. Uitdehaag,[‡,⊥,@] Bart A. van der Veen,[‡,§,+] Bauke W. Dijkstra,[‡,⊥] Marc J. E. C. van der Maarel,[‡,#] and Lubbert Dijkhuizen*[,‡,§]

Centre for Carbohydrate Bioprocessing TNO, University of Groningen, and Microbial Physiology Research Group, Groningen Biomolecular Sciences and Biotechnology Institute, University of Groningen, Kerklaan 30, 9751 NN Haren, The Netherlands, and Innovative Ingredients and Products Department, TNO-Quality of Life, Rouaanstraat 27, 9723 CC Groningen, The Netherlands, and Laboratory of Biophysical Chemistry, Groningen Biomolecular Sciences and Biotechnology Institute, University of Groningen, Nijenborgh 4, 9747 AG Groningen, The Netherlands

Received November 21, 2006; Revised Manuscript Received January 30, 2007

ABSTRACT: Glycoside hydrolase family 77 (GH77) belongs to the α-amylase superfamily (Clan H) together with GH13 and GH70. GH77 enzymes are amylomaltases or 4-α-glucanotransferases, involved in maltose metabolism in microorganisms and in starch biosynthesis in plants. Here we characterized the amylomaltase from the hyperthermophilic bacterium *Thermus thermophilus* HB8 (Tt AMase). Site-directed mutagenesis of the active site residues (Asp293, nucleophile; Glu340, general acid/base catalyst; Asp395, transition state stabilizer) shows that GH77 Tt AMase and GH13 enzymes share the same catalytic machinery. Quantification of the enzyme's transglycosylation and hydrolytic activities revealed that Tt AMase is among the most efficient 4-α-glucanotransferases in the α-amylase superfamily. The active site contains at least seven substrate binding sites, subsites −2 and +3 favoring substrate binding and subsites −3 and +2 not, in contrast to several GH13 enzymes in which subsite +2 contributes to oligosaccharide binding. A model of a maltoheptaose (G7) substrate bound to the enzyme was used to probe the details of the interactions of the substrate with the protein at acceptor subsites +2 and +3 by site-directed mutagenesis. Substitution of the fully conserved Asp249 with a Ser in subsite +2 reduced the activity 23-fold (for G7 as a substrate) to 385-fold (for maltotriose). Similar mutations reduced the activity of α-amylases only up to 10-fold. Thus, the characteristics of acceptor subsite +2 represent a main difference between GH13 amylases and GH77 amylomaltases.

Amylomaltases (EC 2.4.1.25) are intracellular 4-α-glucanotransferases that transfer part of a 1,4-α-D-glucan to an acceptor molecule, such as glucose or another α-1,4-glucan with a free 4-hydroxyl group. These enzymes have been classified as part of glycoside hydrolase family 77 (GH77) (*1*), which forms the α-amylase superfamily together with GH13 and GH70, sharing a similar fold and active site residues (*2*).

Amylomaltases have been found in microorganisms, as well as in plants, where they are known as D-enzymes. In *Escherichia coli*, the enzyme is essential for growth on short malto-oligosaccharides, which are converted into glucose and longer oligosaccharides. The glucose enters the glycolysis pathway, while the longer malto-oligosaccharides are substrates for maltodextrin phosphorylase, yielding glucose 1-phosphate which can be used in various metabolic pathways (*3*, *4*). Nevertheless, the supply of substrates for growth may not be the only function of amylomaltases, since amylomaltase-encoding genes have also been identified in bacteria like *Aquifex aeolicus*, which is not able to grow on α-linked glucans (*5*, *6*). In plants, D-enzyme is involved in starch metabolism, where its precise role is unclear (*7*, *8*), although a role has been implicated in nocturnal maltose metabolism in the cytoplasm (*9*). Amylomaltases can be used for the production of cycloamylose (*10*) and thermoreversible starch gels (*11*), which are both of commercial interest.

The first elucidated three-dimensional (3D) structure of a GH77 enzyme was that of the amylomaltase from *Thermus aquaticus* ATCC33923 (Taq AMase)[1] (*12*). It revealed a catalytic A domain with a TIM barrel fold and inserted B1,

† This research was sponsored in part by the EU 5FP CEGLYC project (Contract QLK3-CT-2001-00149).

* To whom correspondence should be addressed. Telephone: +31-50-3632150. Fax: +31-50-3632154. E-mail: L.Dijkhuizen@rug.nl.

‡ Centre for Carbohydrate Bioprocessing TNO, University of Groningen.

§ Microbial Physiology Research group, Groningen Biomolecular Sciences and Biotechnology Institute (GBB), University of Groningen.

|| Present address: Carnegie Institution, Department of Plant Biology, Stanford University, 260 Panama St., Stanford, CA 94305.

⊥ Laboratory of Biophysical Chemistry, Groningen Biomolecular Sciences and Biotechnology Institute (GBB), University of Groningen.

@ Present address: Organon, Molenstraat 110, P.O. Box 20, 5340 BH Oss, The Netherlands.

+ Present address: GlycoEnzymology Research Group (GRG), INSA, Toulouse, France.

TNO-Quality of Life.

[1] Abbreviations: AMase, amylomaltase; *Bci*251, *Bacillus circulans* 251; CGTase, cyclodextrin glucanotransferase; DP, degree of polymerization; G*n*, α-1,4-oligosaccharide of *n* glucose monomers; Tabium, *Thermoanaerobacterium thermosulfurigenes* EM1; Taq, *Thermus aquaticus* ATCC 33923; Tt, *Thermus thermophilus* HB8; wt, wild-type.

10.1021/bi602408j CCC: $37.00
Published on Web 04/04/2007

B2, and B3 subdomains. A conserved loop of eight amino acid residues, the 250s loop, is partially shielding the active center. Amino acids that interact with the substrate have been identified in the 3D structure of Taq AMase with the inhibitor acarbose bound in the active site at substrate binding subsites −3 to +1 (*13*). In the center of the substrate-binding cleft, two conserved aspartate residues and one glutamate residue were located (*12*), and they correspond to the three catalytic acidic residues in the GH13 enzymes. From this, Asp293 has been proposed to serve as the nucleophile in the α-retaining mechanism, Glu340 may function as the general acid/base catalyst, and Asp395 may stabilize the oxocarbenium ion-like transition state (*12*, *14*, *15*).

GH77 enzymes are efficient 4-α-glucanotransferases and exhibit remarkably low hydrolytic activities that are at least 1 order of magnitude lower than that of cyclodextrin glucanotransferases (CGTases) of GH13 (*16*−*19*), indicating tight control of the reaction course during catalysis. Mutagenesis of residues remote from the active site decreased the hydrolytic activity of GH77 Taq AMase (*16*), but the active site of these enzymes has not been studied in relation to the reaction specificity.

In this study, we show that Tt AMase is a very efficient 4-α-glucanotransferase with one of the highest transglycosylation to hydrolysis ratios in the α-amylase superfamily. By characterizing the disproportionation activity, using inhibition studies, modeling a maltoheptaose substrate in the active site, and using site-directed mutagenesis, we confirmed the roles of the putative catalytic residues and identified acceptor subsites +2 and +3 in the active site. While the main catalytic machinery is the same for GH77 and GH13, the properties of acceptor subsite +2 distinguish the two families.

MATERIALS AND METHODS

Chemicals, Strains, and Vectors. All chemicals were analytical grade. Malto-oligosaccharides were obtained from Sigma-Aldrich (Zwijndrecht, The Netherlands). Food-grade native potato starch was a gift from AVEBE (Veendam, The Netherlands). A sample of acarbose from Bayer (Mijdrecht, The Netherlands) was a gift from T. R. M. Barends (University of Groningen). Oligonucleotides were from Eurogentec (Seraing, Belgium). *E. coli* TOP10 and *E. coli* BL21(DE3) were used as hosts for cloning and protein production, respectively. Vector pET15b (p_{T7}, N-terminal His_6 tag, amp^R) (Novagen, Madison, WI) was used for cloning of mutated amylomaltase (*malQ*) genes.

Purification of Thermus thermophilus Amylomaltase. The *T. thermophilus malQ* gene was cloned into the pET15b vector (pCCBmalQ), which results in a protein with a N-terminal His tag. *E. coli* BL21(DE3)/pCCBmalQ was routinely cultured in 250 mL of LB^+ medium (1% tryptone, 0.5% yeast extract, 0.5% NaCl, and 100 μg/mL ampicillin) at 37 °C while being shaken and purified as described previously (*17*), the difference being that the cell-free extract was incubated at 70 °C for 10 min. Purified Tt AMase was dialyzed against 25 mM sodium phosphate buffer (pH 7.5) and stored at 4 °C. Typically, 20−40 mg of pure Tt AMase protein was obtained per liter of cell culture. The protein concentration was determined according to the Bradford method using the Bio-Rad reagent and bovine serum albumin as a standard.

Construction of Site-Directed Mutants. Mutations were introduced by PCR using the pCCBmalQ plasmid as a template. D249S, D293N, D293A, E340A, D395N, D395A, and F366L mutations were introduced using the megaprime method. The E340Q mutation was introduced using the QuikChange site-directed mutagenesis kit (Stratagene, La Jolla, CA). DNA sequencing was used to verify the sequence of the amplified DNA and to confirm the presence of the desired mutations (BaseClear, Leiden, The Netherlands).

pH Optima. Two buffers were tested for determination of the optimal pH for activity at 70 °C, i.e., 90 mM sodium maleate and 90 mM citrate−phosphate buffer in the pH range of 3.5−7.5 essentially as described previously (*17*). In a vial, 500 μL of 10 mM maltotriose in buffer was preheated for 2 min at 70 °C. After addition of enzyme to a final concentration of 34 nM, glucose formation was followed for 1.5 min by transferring 50 μL samples with a 15 s interval to a 96-well microtiter plate on ice. After addition of 180 μL GOD-PAP glucose detection kit per well (Roche), the 96-well microtiter plate was incubated for 30 min at ambient temperature, and the OD_{490} was determined. A glucose standard curve (0−50 mM) was included in each plate. One unit of activity was defined as the release of 1 μmol of glucose/min. For the Tt AMase variants D293N and E340Q, 100 μL of 10 mM maltotriose in 90 mM combined citrate−phosphate buffer in the pH range of 4.0−7.0 was incubated with 33−50 μM enzyme for 5−15 h at 70 °C. Glucose formation was assessed as described above. Tt AMase D293N and E340Q were active below pH 6.5 and 5.5, respectively, but precipitated during the necessary prolonged incubation times. Wild-type Tt AMase precipitated below pH 5.5 under similar extended incubation times as well, which showed that the D293N mutation reduced the pH stability of the enzyme.

Kinetic Stability. Purified Tt AMase (0.1 mg/mL) in 25 mM sodium citrate and 25 mM sodium phosphate buffer (pH 5.5) was incubated at various temperatures (50−90 °C). After being incubated for 0, 5, 10, 15, 30, 45, 60, 90, 120, and 180 min, samples were removed and stored on ice. Residual activity was determined as described above, and the half-life of inactivation was calculated as described previously (*17*).

Kinetic Analyses. Rates of product formation were analyzed by HPLC. Activity assays were performed as for determination of the pH optimum. Samples (50 μL) were transferred to 450 μL of DMSO at 15 s intervals, which terminated the reaction, and analyzed for products up to G10 by Dionex HPLC as described previously (*17*). Standards were included at the beginning, middle, and end of the detection series to correct for detector drift. The detector response factor for G7 was used for the determination of the concentrations of G8, G9, and G10.

The disproportionation activity was routinely assayed at 70 °C in 25 mM citrate−phosphate buffer at the pH optimum of the respective Tt AMase variant as described previously (*17*). A molecular mass of 59 337 Da was assumed in the calculation of the k_{cat}. The activity of D249S was measured by incubating 425 nM enzyme in 10 mM substrate (G3−G7) in 25 mM citrate−phosphate buffer (pH 5.5) (in triplicate) at 70 °C for 14 h. Subsequently, 50 μL samples were transferred to a 180 μL GOD-PAP glucose detection kit (Roche) and analyzed as described above. Samples incubated without enzyme served as controls.

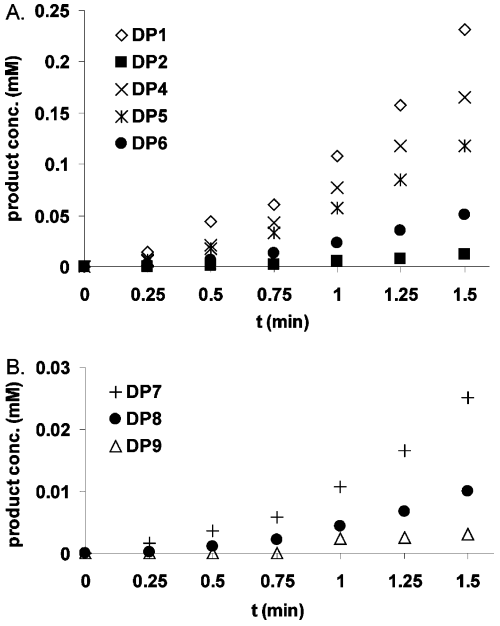

FIGURE 1: Formation of the initial products by 34 nM Tt AMase wt on 10 mM G3 substrate in 25 mM sodium citrate/sodium phosphate (pH 5.5) at 70 °C. Formation of malto-oligosaccharide products of (A) DP1−DP6 and (B) DP7−DP9 is depicted.

Hydrolysis of starch was assessed by incubating (in triplicate) 340 nM Tt AMase variant with 1.0% gelatinized native potato starch in 10 mM maleate buffer (pH 6.5) at 70 °C as described previously (*17*). One unit of hydrolyzing activity was defined as the production of 1 μmol of reducing ends/min.

The inhibitory effect of acarbose on the disproportionation activity of Tt AMase was determined at eight concentrations of maltotriose (0−25 mM) and acarbose concentrations of 25, 50, and 100 μM. Assays were the same as those described for the determination of the optimal pH. Inhibition constants for competitive and uncompetitive binding were calculated by fitting the data to a formula for mixed inhibition (*20*) using SigmaPlot (SPSS Inc., Chicago, IL).

RESULTS

Optimal pH for Activity and Stability of Tt AMase. The activity of Tt AMase was analyzed using maltotriose as a substrate, which is converted into glucose (G1) and malto-oligosaccharides by Tt AMase (see below). At 70 °C, the temperature used for all kinetic analyses, the highest disproportionation activity in combined citrate−phosphate buffer was at pH 5.5−6.0, while it was optimal at pH 6.0−6.5 for sodium maleate. In both buffers, the kinetic parameters were the same for the enzyme. In combined citrate−phosphate buffer (pH 5.5), the enzyme was stable up to 80 °C, where it displayed an activity half-life of 18 ± 4 min (data not shown).

Disproportionation of Malto-Oligosaccharides. At a substrate concentration of 10 mM, the initial rate of formation of disproportionation products was analyzed at 70 °C using malto-oligosaccharides with a degree of polymerization (DP) of 3−7 as substrates (Figures 1 and 2). HPLC analysis showed that Tt AMase wt formed a range of malto-oligosaccharides on all substrates. In the case of maltotriose (G3), products of DP6 and longer resulted from the disproportionation of reaction products. Tt AMase has a higher affinity for the longer reaction products than for G3, since Tt AMase prefers conversion of the longer products to that of the more abundant G3. Product formation rates with G3 as a substrate increased with incubation time and were constant only between 45 and 90 s (Figure 1), which coincided with the formation of products longer than G8. This suggested that the active site of Tt AMase might contain up to nine substrate-binding sites. The increase in the level of product formation was linear for all other substrates (Figure 2). Glucose was produced on all substrates, which means it can serve as an indicator for Tt AMase activity. Disproportionation of malto-oligosaccharides results in the production of equal amounts of two oligosaccharide products that differ in length by twice the transferred saccharide unit. However, for most substrates, a single dominant product was observed. This product is likely to correspond to the saccharide that is released when the covalent enzyme−substrate reaction intermediate is formed, since it has to leave the active site before the bound part of the substrate is released by an incoming acceptor. The preferred binding modes of the initial substrates in the active site of Tt AMase were deduced from the dominant products (Table 1).

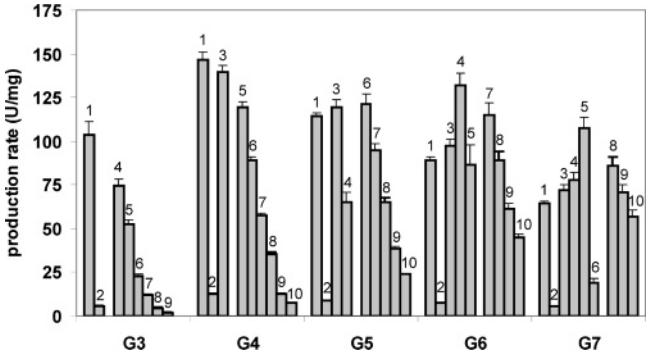

FIGURE 2: Rates of product formation of Tt AMase on 10 mM malto-oligosaccharides. Numbers above the bars correspond to the degree of polymerization of malto-oligosaccharide products. Assays were performed in 25 mM sodium citrate/sodium phosphate (pH 5.5) at 70 °C with 34 nM enzyme. Rates for G3 were determined between the 45 and 90 s points of incubation.

Table 1: Dominant Binding Modes of Substrates in the Active Site of Tt AMase

substrate	−4	−3	−2	−1	+1	+2	+3	+4	+5[a]	product[b]
G3			O	O	Ø					G1
G4		O	O	O	Ø					G1
G4				O	O	O	Ø			G3
G5	O	O	O	O	Ø					G1
G5			O	O	O	O	Ø			G3
G6			O	O	O	O	O	Ø		G4
G7			O	O	O	O	O	O	Ø	G5

[a] The numbering of substrate binding subsites is that of Davies (*55*). The glycosidic linkage is broken between subsites −1 and +1. [b] Product that is released upon formation of the covalent intermediate; Ø, reducing sugar.

No kinetic constants for disproportionation of malto-oligosaccharides by Tt AMase and Taq AMase have been reported. Previously, the disproportionation activities of the cyclodextrin glucanotransferases (CGTases) from *Bacillus circulans* 251 (*Bci*251) and *Thermoanaerobacterium thermosulfurigenes* EM1 (Tabium) have been characterized in detail using the double-blocked substrate 4-nitrophenyl-α-D-maltoheptaoside-4,6-*O*-ethylidene (*21*, *22*). However, Tt

Table 2: Kinetics of the Release of Glucose by Tt AMase wt and Mutants D249S and F366L Incubated with G2−G7 Substrates[a]

	wild type		F366L			D249S[f]	
substrate	K_M (mM)	k_{cat} (s^{-1})	K_M (mM)	k_{cat} (s^{-1})	inactive[g]	k_{cat} (s^{-1})	inactive[h]
G2	ND[b]	6[b]	ND[b]	5[b]		N[e]	
G3	2.2 ± 0.2	317 ± 7[c]	3.3 ± 0.9	111 ± 9	4.2	0.68 ± 0.01	385
G4	5.4 ± 1.6	425 ± 33	2.4 ± 1.5	106 ± 18[d]	1.8	0.97 ± 0.03	298
G5	10.8 ± 1.2	329 ± 12	6.2 ± 1.9	179 ± 18[c]	1.0	3.98 ± 0.09	59
G6	17.4 ± 3.9	304 ± 28	15.5 ± 2.2	188 ± 18	1.4	3.26 ± 0.05	27
G7	14.9 ± 3.4	213 ± 19	15.1 ± 1.5	159 ± 8	1.3	1.99 ± 0.16	23

[a] Assays were performed in 25 mM citrate−phosphate buffer at pH 5.5 and 70 °C. The enzyme concentration used in the assays varied from 34 nM (wild type and F366L) to 170 nM (D249S). [b] Cannot be determined. Data could not be fitted according to Michaelis−Menten kinetics. The highest observed activity is shown. [c] Substrate inhibition above 25 mM. [d] Substrate inhibition above 7.5 mM. [e] Not determined. [f] Activity determined at a substrate concentration of 10 mM. [g] Inactivation rate: $(k_{cat}/K_M)_{wt}/(k_{cat}/K_M)_{F366L}$. [h] Inactivation rate: the activity of Tt AMase wt on 10 mM substrate divided by the activity of D249S.

AMase was not able to convert this compound, nor was it active on the chromogenic substrates *p*-nitrophenol (pNP)-α-D-maltose and pNp-α-D-maltopentaoside (data not shown). Therefore, Tt AMase was incubated with varying concentrations of maltose (G2) to maltoheptaose (G7), and the K_M and k_{cat} for release of glucose were determined (Table 2), which are largely similar to those reported for the amylomaltases from *Pyrobaculum aerophilum* (*17*) and *A. aeolicus* (*6*).

Maltose is a poor substrate for Tt AMase, indicating that substrate binding in only subsites −1 and +1 is insufficient for promotion of catalysis. Maltrotriose (G3) is disproportionated efficiently and yields glucose as a main product, as a result of G3 binding in subsites −2 to +1. Only low levels of maltose are produced from G3, indicating that subsite +2 has a negative effect on binding. The observed maltose production demonstrates that Tt AMase is slightly more versatile in substrate binding than potato D-enzyme and *P. aerophilum* amylomaltase, which do not bind at all the reducing end glucose residue of the substrate in acceptor subsite +2, but rather in acceptor subsite +1 or in subsite +3 (*17*, *23*). Conversion of maltotetraose (G4) had glucose as a main product as well, in agreement with substrate binding at subsites −3 to +1. The 2-fold increased K_M for this binding mode and the relatively high rate of maltose release resulting from binding of G4 at subsites −2 to +2 signify a reduced affinity for substrate binding at subsite −3. In addition, G4 is the only substrate that releases high levels of the product resulting from the substrate occupying subsite −1 as single donor subsite. In this case, G4 is bound at subsites −1 to +3 and G3 is produced. When the substrate length increased beyond DP4, the rates for glucose production decreased with an increase in substrate length and K_M values increased. Maltose was produced at low levels for these substrates as well, indicating that they are preferably bound at the donor subsites and acceptor subsites +1, +2, and +3, and possibly additional acceptor subsites. With maltopentaose (G5) as a substrate, Tt AMase produced G1, G3, and maltohexaose (G6) at almost equal rates (Figure 2), G1 and G3 resulting from initial binding of G5 in two different binding modes (Table 1) and G6 resulting from the disproportionation of a reaction product. Disproportionation production rates of G6 and G7 indicate a preferred binding at donor subsites −1 and −2 with the remainder of the substrate in acceptor subsites. Thus, binding at acceptor subsite +3 and possibly higher acceptor subsites is favored over binding at donor subsite −3.

Hydrolysis of Starch by Tt AMase. Tt AMase is highly active on gelatinized native potato starch, as judged from the color shift of the starch−iodine complex from blue to purple (data not shown). This color shift is due to the transfer of amylose chains to the amylopectin branches (*11*, *24*). However, an increase in reducing ends was also measured, which can be only the result of hydrolysis of amylose chains by a water molecule acting as an acceptor by cleaving the covalent enzyme−substrate intermediate instead of a glucan. Nevertheless, this hydrolytic activity is very low (k_{cat} = 6.0×10^{-2} s^{-1}). The enzyme's disproportionation activity on maltotriose is 317 s^{-1} (Table 2). Since maltotriose was the acceptor in this reaction, it is a 5000-fold better acceptor than water. This high transglycosylation over hydrolysis specificity of amylomaltase is much higher than that of other Clan H enzymes. For instance, it is 10-, 150-, 500-, and 1000-fold higher than that of GH13 *Bci*251 CGTase (*19*), GH13 *Neisseria polysaccharea* amylosucrase (*25*), GH13 Tabium CGTase (*18*), and GH70 *Lactobacillus reuteri* 121 reuteransucrase (*26*), respectively. Thus, Tt AMase is one of the most efficient glucanotransferases in Clan H. This is similar to what has been found for the amylomaltase from *P. aerophilum* (*17*).

Inhibition by Acarbose. HPLC analysis demonstrated that Tt AMase was not able to convert the inhibitor acarbose, either in the absence or in the presence of malto-oligosaccharides (data not shown). For Tt AMase-catalyzed disproportionation of maltotriose, acarbose acted as a strong mixed inhibitor with almost equal competitive and uncompetitive binding constants ($K_{i,comp}$ = 3 μM, and $K_{i,uncomp}$ = 4 μM). This indicates that acarbose is both bound in the active site and at another site. Interestingly, the crystal structure of the Taq AMase−acarbose complex reveals two acarbose binding sites; one acarbose is bound in the active site, and the other is near Tyr54, ∼14 Å from the active site (*13*). However, it is not known how acarbose binding at the latter site affects the enzyme's activity.

Catalytic Residues of Tt AMase. The active site architecture of GH77 Taq AMase shows structural similarities to those of GH13 enzymes (*12*), and several residues are conserved between both families (Figure 3). Among these are the predicted catalytic residues Asp293 (nucleophile, region II), Glu340 (general acid/base catalyst, region III), and Asp395 (third catalytic residue, region IV). To verify the importance of these residues, they were substituted with their respective amide derivative, or with alanine. The mutant enzymes exhibited greatly reduced disproportionation activi-

FIGURE 3: Sequence logos of the four conserved regions of (A) GH13 enzymes [based on 29 CGTase and 37 α-amylase sequences (*Bci*251 CGTase amino acid numbering)] and (B) the corresponding regions in GH77 enzymes (based on 44 GH77 enzyme sequences). Residues with numbers above them interact with the substrate in the respective subsite according to (A) *Bci*251 CGTase complexed with maltononaose (PDB entry 1CXK) (*14*) and (B) a model of maltoheptaose bound to Tt AMase (this study). N, nucleophile; A, general acid/base catalyst; T, transition state stabilizer. Identifiers of the sequences used for construction of the logos are listed in Table S1 of the Supporting Information. Logos were produced using the Weblogo server (http://weblogo.berkeley.edu/logo.cgi).

Table 3: Specific Activities of Tt AMase Catalytic Mutants[a]

	k_{cat} (s^{-1})	relative activity[b]
D293N	2×10^{-2}	7×10^{-5}
D293A	4×10^{-5}	1×10^{-7}
E340Q	6×10^{-3}	2×10^{-5}
E340A	9×10^{-4}	3×10^{-6}
D395N	2×10^{-1}	7×10^{-4}
D395A	6×10^{-4}	2×10^{-6}
wild type	291	1

[a] Disproportionation activities were determined in 25 mM maltotriose in 50 mM sodium maleate at pH 6.5 and 70 °C. The enzyme concentration used in the assays varied between 34 nM and 3.4 μM. [b] The activity of the mutant divided by the activity of the wild type.

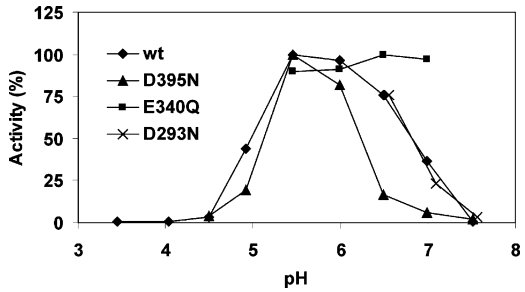

FIGURE 4: Effect of pH on the activity of Tt AMase wt (◆), D293N (×), E340Q (■), and D395N (▲). Tt AMase E340Q and D293N were not stable below pH 5.5 and 6.5, respectively. The activity of D293N has been normalized to the activity of Tt AMase wt at pH 6.5. G1 release was assessed on 10 mM G3 in 90 mM sodium citrate/90 mM NaP_i buffer at 70 °C. The enzyme concentrations were 34 nM (Tt AMase wt) and 33−50 μM (D293N, E340Q, and D395N).

ties (Table 3). Tt AMase D293A was least active, which agrees with the proposed role of Asp293 as a nucleophile in the reaction. Figure 4 shows how the activity of the catalytic amide variants depends on the pH. At pH values above the pH optimum (pH 5.5), the profile of D293N is similar to that of the wild type, while the activity of E340Q is pH-insensitive. This agrees with their predicted roles as a nucleophile and general acid/base catalyst, respectively, for carbohydrate active enzymes that convert substrates via a retaining mechanism (*27*, *28*). The third catalytic residue of GH13 aids in stabilizing the transition state by helping to distort the −1 sugar toward planarity and reducing the electronegativity of the 2-OH group (*14*). In addition, this residue has been suggested to increase the pK_a of the catalytic acid or base residue, thus increasing the optimal pH for activity (*29*). The D395N mutation in AMase is in agreement with this notion since the activity of D395N AMase at higher pH values is reduced compared to that of the wt enzyme (Figure 4).

Model for Substrate Binding in the Active Site of Tt AMase. In GH13 enzymes, acceptor subsites +1, +2, and +3 are important for the course of the catalyzed reaction (*18*). Tt AMase subsites −3 to +1 have been identified in the crystal structure of Taq AMase complexed with acarbose (Figure 5A) (*13*). Several residues that interact with the acarbose glucose residues in subsites −1 and +1 in Taq AMase, including the catalytic residues, are present in three of the four conserved regions (Figure 3). However, in GH77 enzymes, these regions do not seem to contain residues that interact with the substrate in acceptor subsite +2. To identify potential enzyme−substrate interactions in subsites +2 and +3 of GH77 enzymes, a model for substrate binding by Tt AMase was constructed. The modeling was started by superimposing the structure of Taq AMase with bound acarbose (*13*) on that of porcine pancreatic α-amylase with a bound maltohexaose inhibitor (*30*) on the basis of the conserved active site residues of both enzymes. The torsion angles of the glycosidic bonds were adjusted to optimize the fit of the oligosaccharide in the active site of Taq AMase. This modeling was aided by comparisons with the conformations of other oligosaccharides complexed with α-amylase family enzymes, such as maltononaose bound to CGTase (*14*), and a maltohexaose inhibitor bound to Tabium CGTase (*18*). The final model with an oligosaccharide bound from subsite −4 to +3 is schematically shown in Figure 5B. The sugar residues at subsites −1 to +2 have a conformation similar to that which was observed in Tabium CGTase with a maltohexaose inhibitor in the active site (*18*). In contrast, the residues at subsites −4 to −2 have a more linear, extended conformation than those in Tabium CGTase, which are poised to form a cyclodextrin molecule. For comparison, Figure 5C shows the binding of a maltohexaose inhibitor in subsites −3 to + 3 in Tabium CGTase (*31*).

Asp249 and Phe366 in Acceptor Subsites +2 and +3. The model predicted that Asp249 and Phe366 in putative acceptor subsites +2 and +3 interact with the substrate (Figure 5B). Therefore, these residues were analyzed by site-directed mutagenesis to test their role in substrate binding and catalysis. The D249S mutation at subsite +2 resulted in a 23−385-fold reduced glucose liberation activity (Table 2), which disabled further kinetic characterization. The hydrolytic activity of this mutant on potato starch was too low to be detected. Thus, Asp249 is important for catalysis by Tt AMase. The F366L substitution in subsite +3 had a less severe effect on Tt AMase activity. The starch hydrolase activity of this mutant was 4.0×10^{-2} s^{-1}, which is comparable to that of the wild-type enzyme (6.0×10^{-2} s^{-1}). The k_{cat}/K_M of the F366L mutant was most decreased for the conversion of G3, while it was similar to that of the wild type for the disproportionation of G4−G7 (Table 2). Interestingly, there is a difference in substrate inhibition between the wild-type enzyme and the F366L mutant. Wild-type Tt AMase is most active on G3, but it is inhibited above 25

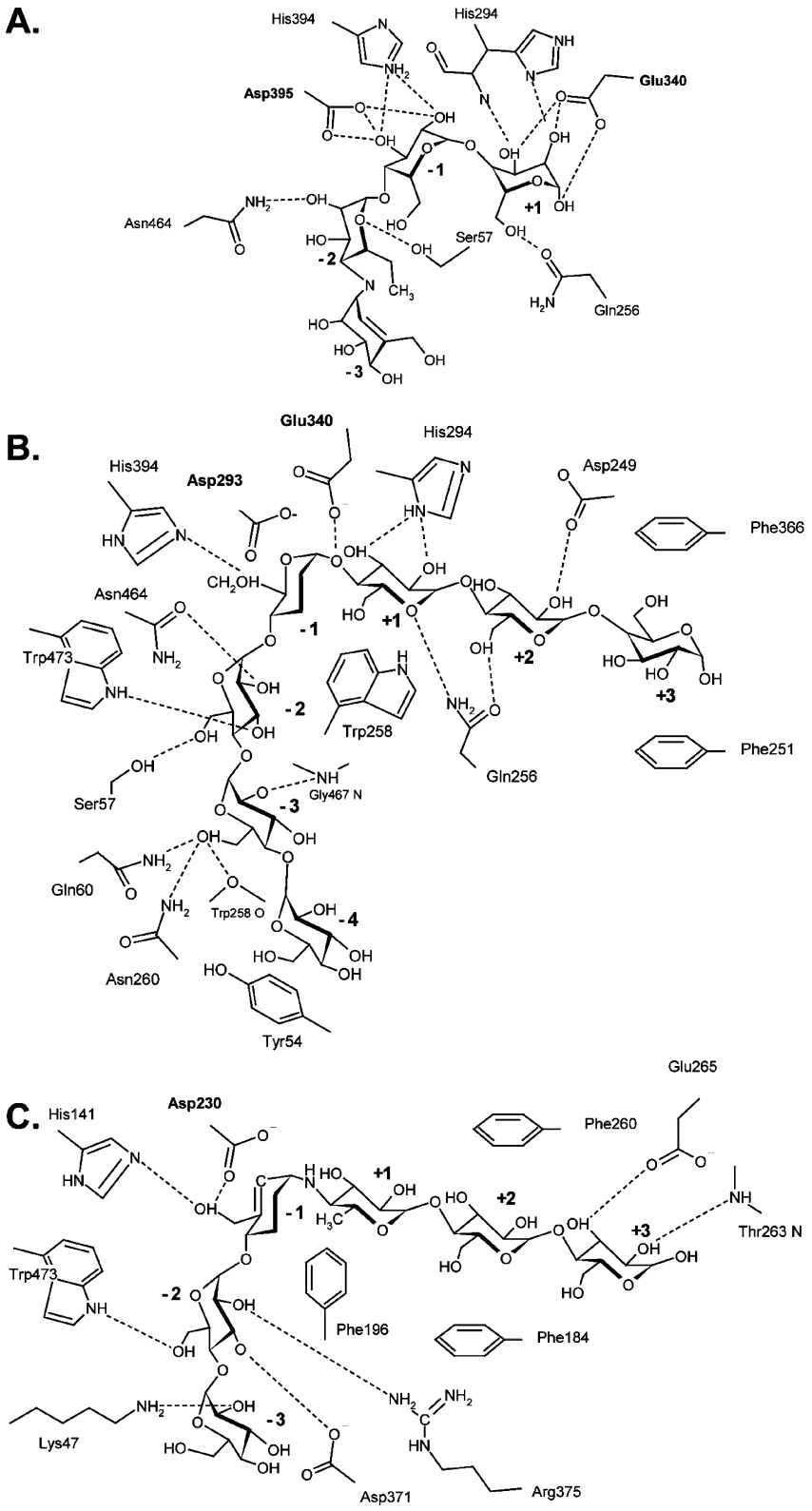

FIGURE 5: Schematic overviews of (A) binding of acarbose in the active site of Taq AMase (PDB entry 1ESW, modified from ref *13*), (B) proposed binding of maltoheptaose in the active site of Taq AMase, and (C) binding of a maltohexaose inhibitor in the active site of Tabium CGTase (PDB entry 1A47). Not all interactions are shown for clarity (modified from ref *31*). Catalytic residues are shown in boldface. The binding of the maltohexaose inhibitor in Tabium CGTase is compared to the proposed model for substrate binding in Taq AMase, since it is the only structure demonstrating sugar binding in acceptor subsite +3.

mM G3 (the activity at 50 mM maltotriose was 75% of k_{cat}). Instead, the F366L mutant is most active on G4 and is severely inhibited above 7.5 mM G4 (activity at 50 mM G4 was 0). Thus, the F366L substitution abolished the G3 substrate inhibition observed for wild-type Tt AMase but introduced G4 substrate inhibition. This indicates that subsite +3 is indeed involved in substrate binding. As such, the characteristics of the D249S and F366L mutants support the

proposed model for substrate binding in acceptor subsites +2 and +3.

DISCUSSION

Glycoside hydrolase family 77 contains 4-α-glucanotransferases and is a member of Clan H, to which family 13 α-amylases and family 70 glucansucrases also belong (*1*). As opposed to those of α-amylases, structure−function relationships of the GH77 enzymes have been little studied, although the 3D structure of the amylomaltase from *T. aquaticus* (Taq AMase) has been determined (*12*). The amylomaltases from *T. thermophilus* (Tt AMase) and *T. aquaticus* (Taq AMase) differ at position 27 with a glutamine and arginine residue, respectively, which are solvent-exposed and are located on the opposite side of the enzyme from the active site. As a consequence, the biochemical properties of Tt AMase are very similar to those reported for Taq AMase (*16*, *32*). Therefore, Tt AMase and Taq AMase will be regarded as the same enzyme in this discussion.

Tt AMase produces the same range of products upon incubation with malto-oligosaccharide substrates as several other GH77 enzymes (*6*, *32*, *33*). The substrate binding modes determined for Tt AMase are similar to those determined for potato D-enzyme (*23*). The kinetics of product formation by Tt AMase shown in Figure 1 also correspond well to the production of even- and odd-numbered malto-oligosaccharides predicted from an in silico simulation of the disproportionation of maltotriose by D-enzyme (*34*). At least seven and possibly up to nine substrate binding subsites contribute to catalysis in Tt AMase. As for barley and salivary amylase, Tt AMase subsite −2 is favored in substrate binding (*35*, *36*), while the unfavorable binding affinity of donor subsite −3 is present in barley amylase as well (*36*). However, acceptor subsites +2 and +3, which have a negative and positive effect on substrate binding, respectively, are different compared to those of the two amylases (*35*, *36*). In addition, the +2 subsites of human pancreatic amylase and Tabium CGTase favor substrate binding as well (*22*, *37*), which focused our attention on Tt AMase acceptor subsites +2 and +3.

The pseudotetrasaccharide acarbose is a potent inhibitor of enzymes of the α-amylase family. The inhibitory moiety of acarbose is acarviosine, which mimics the transition state of the reaction, and is expected to bind at subsites −1 and +1 (*28*). Indeed, acarbose, which consists of an acarviosine unit with a maltose unit attached to its reducing end, has been found to bind at subsites −1 to +3 in the crystal structures of enzyme−acarbose complexes of α-amylases from *Aspergillus oryzae* (PDB entry 7TAA) (*38*), pig pancreas (PDB entry 1CPU) (*37*), *Bacillus liquefaciens* (PDB entry 1E3Z) (*39*), and barley (PDB entry 1BG9) (*40*), and in the complexes with acarbose of Bci251 CGTase (PDB entry 1DTU) (*41*) and Tabium CGTase (PDB entry 1A47) (*31*). Acarbose inhibits the activity of these enzymes with inhibition constants in the micromolar range (0.1−270 μM) (*22*, *42*−*44*), similar to the values obtained for Tt AMase. Nevertheless, in the Taq AMase−acarbose complex, acarbose binds at subsites −3 to +1 (*13*) instead of at subsites −1 to +3, and therefore, acarbose inhibits the enzyme most likely as a ground state inhibitor. Possibly, this binding at subsites −3 to +1 is a result of the unfavorable substrate binding at acceptor subsite +2. Thus, identification of acceptor binding sites +2 and +3 in Tt AMase by modeling of a malto-oligosaccharide substrate in the active site appeared to be desirable.

Substitution of Asp293, Glu340, and Asp395 and analysis of their pH profiles confirmed their function in catalysis as the nucleophile, general acid or base, and transition state stabilizer, respectively. The substitutions yielded enzymes with low but detectable activities, similar to the activities of GH13 enzymes mutated in the equivalent residues (*45*−*47*). It may seem surprising that even when the catalytic nucleophile is mutated, some residual activity is observed. Several explanations can be given for this observation. First, the residual activity may be caused by a low degree of spontaneous deamidation of the Asp293Asn mutant (see, e.g., ref *48*). Second, destabilization of the substrate residue bound in subsite −1 may allow it to react directly with an incoming acceptor even in the absence of the nucleophilic Asp. This property has been exploited in the design of artificial "glycosynthases" (*49*, *50*). Finally, the residual activity may result from errors in translation and protein synthesis (*51*).

We showed that the basic catalytic machinery of GH77 and GH13 enzymes is the same. Therefore, we assumed that substrate binding in Tt AMase and GH13 enzymes is similar. Modeling of a maltoheptaose in the Tt AMase active site on the basis of GH13−enzyme−inhibitor structures allowed the identification of acceptor binding subsites +2 and +3, which was confirmed by substitution of Asp249 and Phe366. This implicated the 250s loop, which is unique to GH77 enzymes, in substrate binding (*12*). Asp249, Gln256, and Trp258 in this loop are fully conserved residues in GH77 sequences and interact with the substrate according to the model.

The reduction of the disproportionation activity of Tt AMase F366L is comparable to that caused by the E264A mutation in acceptor subsite +3 of *Bci*251 CGTase (*52*), indicating that subsite +3 has similar properties in both enzymes. On the other hand, we found that Tt AMase activity relies more on acceptor subsite +2 than on subsite +3. The D249S substitution reduced Tt AMase activity to a larger extent than similar substitutions in barley and salivary amylases (*53*, *54*) or Tabium CGTase (*18*), indicating that the role of subsite +2 in catalysis is more important in Tt AMase than in GH13 enzymes.

Tt AMase was found to be a highly active enzyme with at least seven and possibly up to nine substrate binding sites that readily acts on its products. The enzyme exhibited the high 4-α-glucanotransferase versus hydrolase activity that is characteristic of GH77 amylomaltases. We identified acceptor subsites +2 and +3 by modeling a substrate in the active site and found that the main differences between GH77 and GH13 enzymes are centered at acceptor subsite +2. This subsite is unfavorable for substrate binding in Tt AMase, but D249 at this site is important for activity and implies that the conserved residues in the 250s loop are necessary for the disproportionation of malto-oligosaccharides by GH77 enzymes.

SUPPORTING INFORMATION AVAILABLE

Amino acid sequence identifiers used for construction of sequence logos in Figure 3. This material is available free of charge via the Internet at http://pubs.acs.org.

REFERENCES

1. Coutinho, P. M., and Henrissat, B. (1999) Carbohydrate-active enzymes: An integrated database approach, in *Recent Advances in Carbohydrate Bioengineering* (Gilbert, H. J., Davies, G., Henrissat, B., and Svensson, B., Eds.) pp 3−12, The Royal Society of Chemistry, Cambridge, England.
2. MacGregor, E. A., Janecek, S., and Svensson, B. (2001) Relationship of sequence and structure to specificity in the α-amylase family of enzymes, *Biochim. Biophys. Acta 1546*, 1−20.
3. Boos, W., and Shuman, H. (1998) Maltose/maltodextrin system of *Escherichia coli*: Transport, metabolism, and regulation, *Microbiol. Mol. Biol. Rev. 62*, 204−229.
4. Schinzel, R., and Nidetzky, B. (1999) Bacterial α-glucan phosphorylases, *FEMS Microbiol. Lett. 171*, 73−79.
5. Deckert, G., Warren, P. V., Gaasterland, T., Young, W. G., Lenox, A. L., Graham, D. E., Overbeek, R., Snead, M. A., Keller, M., Aujay, M., Huber, R., Feldman, R. A., Short, J. M., Olsen, G. J., and Swanson, R. V. (1998) The complete genome of the hyperthermophilic bacterium *Aquifex aeolicus*, *Nature 392*, 353−358.
6. Bhuiyan, S. H., Kitaoka, M., and Hayashi, K. (2003) A cycloamylose-forming hyperthermostable 4-α-glucanotransferase of *Aquifex aeolicus* expressed in *Escherichia coli*, *J. Mol. Catal. B: Enzym. 22*, 45−53.
7. Colleoni, C., Dauville, D., Mouille, G., Bulon, A., Gallant, D., Bouchet, B., Morell, M., Samuel, M., Delrue, B., d'Hulst, C., Bliard, C., Nuzillard, J. M., and Ball, S. (1999) Genetic and biochemical evidence for the involvement of α-1,4-glucanotransferases in amylopectin synthesis, *Plant Physiol. 120*, 993−1004.
8. Critchley, J. H., Zeeman, S. C., Takaha, T., Smith, A. M., and Smith, S. M. (2001) A critical role for disproportionating enzyme in starch breakdown is revealed by a knock-out mutation in *Arabidopsis*, *Plant J. 26*, 89−100.
9. Chia, T., Thorneycroft, D., Chapple, A., Messerli, G., Chen, J., Zeeman, S. C., Smith, S. M., and Smith, A. M. (2004) A cytosolic glucosyltransferase is required for conversion of starch to sucrose in *Arabidopsis* leaves at night, *Plant J. 37*, 853−863.
10. Takaha, T., Yanase, M., Takata, H., Okada, S., and Smith, S. M. (1996) Potato D-enzyme catalyzes the cyclization of amylose to produce cycloamylose, a novel cyclic glucan, *J. Biol. Chem. 271*, 2902−2908.
11. Van der Maarel, M. J. E. C., Caprona, I., Euverink, G. J. W., Bos, H. T. P., Kaper, T., Binnema, D. J., and Steeneken, P. (2005) A novel thermoreversible gelling product made by enzymatic modification of starch, *Starch 57*, 465−472.
12. Przylas, I., Tomoo, K., Terada, Y., Takaha, T., Fujii, K., Saenger, W., and Strater, N. (2000) Crystal structure of amylomaltase from *Thermus aquaticus*, a glycosyltransferase catalysing the production of large cyclic glucans, *J. Mol. Biol. 296*, 873−886.
13. Przylas, I., Terada, Y., Fujii, K., Takaha, T., Saenger, W., and Strater, N. (2000) X-ray structure of acarbose bound to amylomaltase from *Thermus aquaticus*. Implications for the synthesis of large cyclic glucans, *Eur. J. Biochem. 267*, 6903−6913.
14. Uitdehaag, J. C. M., Mosi, R., Kalk, K. H., van der Veen, B. A., Dijkhuizen, L., Withers, S. G., and Dijkstra, B. W. (1999) X-ray structures along the reaction pathway of cyclodextrin glycosyltransferase elucidate catalysis in the α-amylase family, *Nat. Struct. Biol. 6*, 432−436.
15. Uitdehaag, J. C. M., Van der Veen, B. A., Dijkhuizen, L., and Dijkstra, B. W. (2002) Catalytic mechanism and product specificity of cyclodextrin glycosyltransferase, a prototypical transglycosylase from the α-amylase family, *Enzyme Microb. Technol. 30*, 295−304.
16. Fujii, K., Minagawa, H., Terada, Y., Takaha, T., Kuriki, T., Shimada, J., and Kaneko, H. (2005) Use of random and saturation mutageneses to improve the properties of *Thermus aquaticus* amylomaltase for efficient production of cycloamyloses, *Appl. Environ. Microbiol. 71* (10), 5823−5827.
17. Kaper, T., Talik, B., Ettema, T. J., Bos, H., Van der Maarel, M. J. E. C., and Dijkhuizen, L. (2005) The amylomaltase of *Pyrobaculum aerophilum* IM2 produces thermo-reversible starch gels, *Appl. Environ. Microbiol. 71*, 5098−5106.
18. Leemhuis, H., Dijkstra, B. W., and Dijkhuizen, L. (2002) Mutations converting cyclodextrin glycosyltransferase from a transglycosylase into a starch hydrolase, *FEBS Lett. 514*, 189−192.
19. Leemhuis, H., Uitdehaag, J. C. M., Rozeboom, H. J., Dijkstra, B. W., and Dijkhuizen, L. (2002) The remote substrate binding subsite −6 in cyclodextrin-glycosyltransferase controls the transferase activity of the enzyme via an induced-fit mechanism, *J. Biol. Chem. 277*, 1113−1119.
20. Cornish-Bowden, A. (1999) *Fundamentals of enzyme kinetics*, Portland Press, Cambridge, England.
21. Van der Veen, B. A., Van Alebeek, G. J., Uitdehaag, J. C. M., Dijkstra, B. W., and Dijkhuizen, L. (2000) The three transglycosylation reactions catalyzed by cyclodextrin glycosyltransferase from *Bacillus circulans* (strain 251) proceed via different kinetic mechanisms, *Eur. J. Biochem. 267*, 658−665.
22. Leemhuis, H., Dijkstra, B. W., and Dijkhuizen, L. (2003) *Thermoanaerobacterium thermosulfurigenes* cyclodextrin glycosyltransferase, *Eur. J. Biochem. 270*, 155−162.
23. Jones, G., and Whelan, W. J. (1969) The action pattern of D-enzyme, a transmaltodextrinylase from potato, *Carbohydr. Res. 9*, 483−490.
24. Bates, F. L., French, D., and Rundle, R. E. (1943) Amylose and amylopectin content of starches determined by their iodine complex formation, *J. Am. Chem. Soc. 65*, 142−148.
25. Albenne, C., Skov, L. K., Mirza, O., Gajhede, M., Feller, G., D'Amico, S., Andrâe, G., Potocki-Vâeronáese, G., van der Veen, B. A., Monsan, P., and Remaud-Simeon, M. (2004) Molecular basis of the amylose-like polymer formation catalyzed by *Neisseria polysaccharea* amylosucrase, *J. Biol. Chem. 279*, 726−734.
26. Kralj, S., van Geel-Schutten, G. H., van der Maarel, M. J., and Dijkhuizen, L. (2004) Biochemical and molecular characterization of *Lactobacillus reuteri* 121 reuteransucrase, *Microbiology 150*, 2099−2112.
27. McIntosh, L. P., Hand, G., Johnson, P. E., Joshi, M. D., Korner, M., Plesniak, L. A., Ziser, L., Wakarchuk, W. W., and Withers, S. G. (1996) The pKa of the general acid/base carboxyl group of a glycosidase cycles during catalysis: A ^{13}C-NMR study of *Bacillus circulans* xylanase, *Biochemistry 35*, 9958−9966.
28. Mosi, R., Sham, H., Uitdehaag, J. C. M., Ruiterkamp, R., Dijkstra, B. W., and Withers, S. G. (1998) Reassessment of acarbose as a transition state analogue inhibitor of cyclodextrin glycosyltransferase, *Biochemistry 37*, 17192−17198.
29. Strokopytov, B., Penninga, D., Rozeboom, H. J., Kalk, K. H., Dijkhuizen, L., and Dijkstra, B. W. (1995) X-ray structure of cyclodextrin glycosyltransferase complexed with acarbose. Implications for the catalytic mechanism of glycosidases, *Biochemistry 34*, 2234−2240.
30. Machius, M., Vertesy, L., Huber, R., and Wiegand, G. (1996) Carbohydrate and protein-based inhibitors of porcine pancreatic α-amylase: Structure analysis and comparison of their binding characteristics, *J. Mol. Biol. 260*, 409−421.
31. Wind, R. D., Uitdehaag, J. C. M., Buitelaar, R. M., Dijkstra, B. W., and Dijkhuizen, L. (1998) Engineering of cyclodextrin product specificity and pH optima of the thermostable cyclodextrin glycosyltransferase from *Thermoanaerobacterium thermosulfurigenes* EM1, *J. Biol. Chem. 273*, 5771−5779.
32. Terada, Y., Fujii, K., Takaha, T., and Okada, S. (1999) *Thermus aquaticus* ATCC 33923 amylomaltase gene cloning and expression and enzyme characterization: Production of cycloamylose, *Appl. Environ. Microbiol. 65*, 910−915.
33. Takaha, T., Yanase, M., Okada, S., and Smith, S. M. (1993) Disproportionating enzyme (4-α-glucanotransferase; EC 2.4.1.25) of potato. Purification, molecular cloning, and potential role in starch metabolism, *J. Biol. Chem. 268*, 1391−1396.
34. Nakatani, H. (1999) Monte Carlo simulation of 4-α-glucanotransferase reaction, *Biopolymers 50*, 145−151.
35. Kandra, L., Gyâemâant, G., Remenyik, J., Ragunath, C., and Ramasubbu, N. (2003) Subsite mapping of human salivary α-amylase and the mutant Y151M, *FEBS Lett. 544*, 194−198.
36. Kandra, L., Hachem, M. A., Gyemant, G., Kramhoft, B., and Svensson, B. (2006) Mapping of barley α-amylases and outer subsite mutants reveals dynamic high-affinity subsites and barriers in the long substrate binding cleft, *FEBS Lett. 580*, 5049−5053.
37. Brayer, G. D., Sidhu, G., Maurus, R., Rydberg, E. H., Braun, C., Wang, Y., Nguyen, N. T., Overall, C. M., and Withers, S. G. (2000) Subsite mapping of the human pancreatic α-amylase active site through structural, kinetic, and mutagenesis techniques, *Biochemistry 39*, 4778−4791.
38. Brzozowski, A. M., and Davies, G. J. (1997) Structure of the *Aspergillus oryzae* α-amylase complexed with the inhibitor acarbose at 2.0 Å resolution, *Biochemistry 36*, 10837−10845.
39. Brzozowski, A. M., Lawson, D. M., Turkenburg, J. P., Bisgaard-Frantzen, H., Svendsen, A., Borchert, T. V., Dauter, Z., Wilson, K. S., and Davies, G. J. (2000) Structural analysis of a chimeric

bacterial α-amylase. High-resolution analysis of native and ligand complexes, *Biochemistry 39*, 9099−9107.
40. Kadziola, A., Sogaard, M., Svensson, B., and Haser, R. (1998) Molecular structure of a barley α-amylase-inhibitor complex: Implications for starch binding and catalysis, *J. Mol. Biol. 278*, 205−217.
41. Van der Veen, B. A., Uitdehaag, J. C. M., Penninga, D., van Alebeek, G. J., Smith, L. M., Dijkstra, B. W., and Dijkhuizen, L. (2000) Rational design of cyclodextrin glycosyltransferase from *Bacillus circulans* strain 251 to increase α-cyclodextrin production, *J. Mol. Biol. 296*, 1027−1038.
42. Kim, M. J., Lee, S. B., Lee, H. S., Lee, S. Y., Baek, J. S., Kim, D., Moon, T. W., Robyt, J. F., and Park, K. H. (1999) Comparative study of the inhibition of α-glucosidase, α-amylase, and cyclomaltodextrin glucanosyltransferase by acarbose, isoacarbose, and acarviosine-glucose, *Arch. Biochem. Biophys. 371*, 277−283.
43. Oudjeriouat, N., Moreau, Y., Santimone, M., Svensson, B., Marchis-Mouren, G., and Desseaux, V. (2003) On the mechanism of α-amylase, *Eur. J. Biochem. 270*, 3871−3879.
44. Yoon, S. H., and Robyt, J. F. (2003) Study of the inhibition of four α-amylases by acarbose and its 4-α-maltohexaosyl and 4-α-maltododecaosyl analogues, *Carbohydr. Res. 338*, 1969−1980.
45. Knegtel, R. M., Strokopytov, B., Penninga, D., Faber, O. G., Rozeboom, H. J., Kalk, K. H., Dijkhuizen, L., and Dijkstra, B. W. (1995) Crystallographic studies of the interaction of cyclodextrin glycosyltransferase from *Bacillus circulans* strain 251 with natural substrates and products, *J. Biol. Chem. 270*, 29256−29264.
46. Rydberg, E. H., Li, C., Maurus, R., Overall, C. M., Brayer, G. D., and Withers, S. G. (2002) Mechanistic analyses of catalysis in human pancreatic α-amylase: Detailed kinetic and structural studies of mutants of three conserved carboxylic acids, *Biochemistry 41*, 4492−4502.
47. Svensson, B. (1994) Protein engineering in the α-amylase family: Catalytic mechanism, substrate specificity, and stability, *Plant Mol. Biol. 25*, 141−157.
48. Reissner, K. J., and Aswad, D. W. (2003) Deamidation and isoaspartate formation in proteins: Unwanted alterations or surreptitious signals? *Cell. Mol. Life Sci. 60*, 1281−1295.
49. Mackenzie, L. F., Wang, Q., Warren, R. A. J., and Withers, S. G. (1998) Glycosynthases: Mutant glycosidases for oligosaccharide synthesis, *J. Am. Chem. Soc. 120*, 5583−5584.
50. Okuyama, M., Mori, H., Watanabe, K., Kimura, A., and Chiba, S. (2002) α-Glucosidase mutant catalyzes "α-glycosynthase"-type reaction, *Biosci., Biotechnol., Biochem. 66* (4), 928−933.
51. Fersht, A. (1999) *Structure and mechanism in protein science*, W. H. Freeman and Company, New York.
52. Van der Veen, B. A., Leemhuis, H., Kralj, S., Uitdehaag, J. C. M., Dijkstra, B. W., and Dijkhuizen, L. (2001) Hydrophobic amino acid residues in the acceptor binding site are main determinants for reaction mechanism and specificity of cyclodextrin-glycosyltransferase, *J. Biol. Chem. 276*, 44557−44562.
53. Matsui, I., and Svensson, B. (1997) Improved activity and modulated action pattern obtained by random mutagenesis at the fourth β-α loop involved in substrate binding to the catalytic $(\beta/\alpha)_8$-barrel domain of barley α-amylase 1, *J. Biol. Chem. 272*, 22456−22463.
54. Mishra, P. J., Ragunath, C., and Ramasubbu, N. (2002) The mechanism of salivary amylase hydrolysis: Role of residues at subsite S2′, *Biochem. Biophys. Res. Commun. 292*, 468−473.
55. Davies, G. J., Wilson, K. S., and Henrissat, B. (1997) Nomenclature for sugar-binding subsites in glycosyl hydrolases, *Biochem. J. 321*, 557−559.

BI602408J